halves, needed for binding a larger bridging ligand, would be as readily or more readily achieved than the "closed" conformation observed in $Fe_2(\mu\text{-}O)(FF)\cdot H_2O$. In particular, the separation of 6.4 Å between planes required[11] for a bridging imidazolate should be readily achieved.

Cytochrome Oxidase Relevance. The mixed-metal species $[MnCo(Im)(FF)]^-$ (**11**) is a good spin model for cytochrome oxidase.[7] Not only does it have interacting first-row transition-metal centers with $S = {}^5/_2$ and $S = {}^1/_2$ spin states like heme a_3 and Cu_B but also it has its unpaired electrons in an orbital orientation which is likely to exist in cytochrome oxidase. High-spin Mn(II) is isoelectronic with high-spin Fe(III) both having single occupation of all five 3d orbitals. Cobalt(II) is low spin having one unpaired electron in the d_{z^2} orbital, an antibonding orbital of σ symmetry with respect to Co–Im bonding. If present in an oxidase, an imidazolate ligand to Cu_B[11] is likely to be the strongest field ligand[11] and therefore, by the fundamental premise of ligand field theory, would have the unpaired electron of the d^9 copper(II) ion in an orbital which is σ antibonding with respect to Cu–Im bonding. Thus, complex **11** would seem to be set up to maximize the antiferromagnetic coupling. But the measured value of $-J$ is only 5 cm^{-1}. This leads to the conclusion that a heme–Im–Cu structure like that envisaged for cytochrome oxidase is very unlikely to have $-J \geq 200\ cm^{-1}$. Solution EPR studies on a proposed Fe–(2-MeIm)–Cu system are also consistent with very weak interactions.[35] The present range of $-J$ for all known imidazolate-bridged species is 0–90 cm^{-1}, so it is unlikely that histidine is providing a bridging ligand to Cu_B at the heme a_3 site of cytochrome oxidase. Other ligands which bring the metals closer together and which are known to mediate stronger antiferromagnetic coupling must be considered.

The structure of $Fe_2(\mu\text{-}O)(FF)$ is suggestive of an oxo-bridged Fe–O–Cu moiety in cytochrome oxidase, and we have adopted this as an alternative working hypothesis to the imidazolate model.[7] Oxygen-bridged moieties, in one form or another, have been frequently postulated in mechanisms involving oxygen reduction at dinuclear metal sites,[36] and the synthetic challenge of preparing heterobinuclear bridged oxo species seems worthy of future effort.

Acknowledgment. We are most grateful to Dr. Frank DiSalvo for variable-temperature magnetic susceptibility measurements and helpful discussions of the results. The work was supported by the National Institutes of Health, Grant GM 23851 to C.A.R. and Grant HL 15627 to W.R.S. J.T.L. was the recipient of an IntraScience Foundation Award. C.A.R. is a Camille and Henry Dreyfus Teacher-Scholar Awardee (1976–1981).

Supplementary Material Available: Table I, giving molar susceptibility and magnetic moment data for complexes **5**, **8**, **9**, and **11**, Table V, root-mean-square displacements of the atoms, a table of observed and calculated structure factor amplitudes (×10), and Table VIII, final group parameters and derived atomic coordinates for the toluene molecules (47 pages). Ordering information is given on any current masthead page.

---

(35) Prosperi, T.; Tomlinson, A. A. G. *J. Chem. Soc., Chem. Commun.* **1979**, 196–197.

(36) (a) Winfield, M. E. *Oxidases and Related Redox Systems, Proc. Symp.* **1965**, *1*, 115–130. (b) Bennet, L. E. *Prog. Inorg. Chem.* **1973**, *18*, 1–176. (c) Chance, B.; Saronio, C.; Leigh, J. S. *Proc. Natl. Acad. Sci. U.S.A.* **1975**, *72*, 1635–1640. (d) Blumberg, W. E.; Peisach, J. In "Cytochrome Oxidase"; King, T. E., Ed.; Elsevier/North-Holland Biomedical Press: Amsterdam, 1979; 153–159. (e) Wilson, D. F.; Erecińska, M. *Ibid.*, 315–318. (f) Caughey, W. S.; Wallace, W. J.; Volpe, J. A.; Yoshikawa, S. In "The Enzymes"; Boyer, P. D., Ed.; Academic Press: New York, 1976; Vol XIII, pp 299–344.

Migratory Insertion Reactions of Carbenes. Kinetics and Mechanism of Migratory Insertion Reactions of Zirconoxy Carbene Complexes of Niobocene Hydride and Alkyls

Richard S. Threlkel[1] and John E. Bercaw*[2]

Contribution No. 6272 from the Arthur Amos Noyes Laboratory of Chemical Physics, California Institute of Technology, Pasadena, California 91125. *Received July 21, 1980*

Abstract: Zirconoxy carbene complexes of niobocene hydride, phenyl, and alkyls, $(\eta^5\text{-}C_5H_5)_2(R)Nb{=}CHOZr(H)(\eta^5\text{-}C_5Me_5)_2$ ($R = H, CH_3, CH_2C_6H_5, CH_2C_6H_4OCH_3, C_6H_5, CH_2OZr(H)(\eta^2\text{-}C_5Me_5)_2$), are prepared via treatment of the corresponding niobocene carbonyls $(\eta^5\text{-}C_5H_5)_2Nb(CO)R$ with $(\eta^5\text{-}C_5Me_5)_2ZrH_2$. For R = H the rate ($30.9 \pm 1.8\ s^{-1}$ at 32.5 °C) of tautomerization to $(\eta^5\text{-}C_5H_5)_2NbCH_2OZr(H)(\eta^5\text{-}C_5Me_5)_2$ was measured by using spin-saturation-transfer techniques (^1H NMR). The rates for alkyl migration to the zirconoxy carbene were obtained from the kinetics of the reactions with diphenylacetylene at 50 °C yielding $(\eta^5\text{-}C_5H_5)_2Nb(H)(PhC{\equiv}CPh)$ and the corresponding *trans*-enolate hydride complexes of bis(pentamethylcyclopentadienyl)zirconium(IV) $(\eta^5\text{-}C_5Me_5)_2Zr(H)(OCH{=}CHR')$. The relative migratory aptitudes ($H \gg CH_3 > CH_2C_6H_6OCH_3 > CH_2C_6H_5$) are discussed.

Introduction

The reduction of carbon monoxide by transition-metal hydrides is an area of intense current interest. We have been investigating the mechanism of CO hydrogenation with carbonyl and hydride derivatives of bis(pentamethylcyclopentadienyl)zirconium. Our findings are discussed in a recent review.[3] A key unsettled issue concerns the molecularity of the initial hydride transfer to the carbonyl ligand of $Cp^*{}_2ZrH_2(CO)$ ($Cp^* = \eta^5\text{-}C_5(CH_3)_5$) (**2**). Two plausible possibilities are (a) intramolecular insertion of CO into a Zr–H bond to yield $Cp^*{}_2Zr(H)(\eta^2\text{-}CHO)$ (**3**) which is subsequently reduced by $Cp^*{}_2ZrH_2$ (**1**) to $Cp^*{}_2(H)ZrCH_2OZr(H)Cp^*{}_2$

---

[1] Fannie and John Hertz Foundation Fellow, 1977–1980.

[2] Camille and Henry Dreyfus Teacher-Scholar, 1977–1982.

(3) (a) Manriquez, J. M.; McAlister, D. R.; Sanner, R. D.; Bercaw, J. E. *J. Am. Chem. Soc.* **1976**, *98*, 6733. (b) Wolczanski, P. T.; Bercaw, J. E. *Acc. Chem. Res.* **1980**, *13*, 121.

0002-7863/81/1503-2650$01.25/0

Scheme I

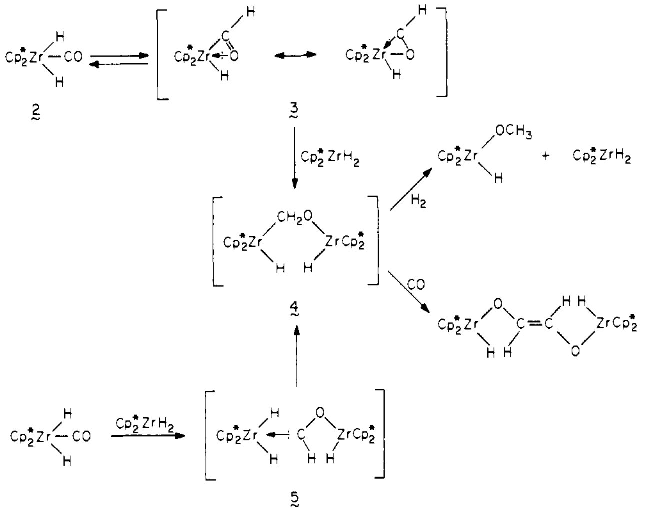

Scheme II

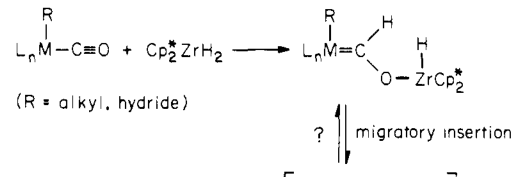

(4) and (b) bimolecular hydride transfer from $Cp^*_2ZrH_2$ (**1**) directly to the carbonyl of $Cp^*_2ZrH_2(CO)$ (**2**) to afford the "zirconoxy carbene" $Cp^*_2(H)_2Zr{=}CHOZr(H)Cp^*_2$ (**5**) which subsequently rearranges to the same intermediate $Cp^*_2(H)ZrCH_2OZr(H)Cp^*_2$ (**4**) (Scheme I). We have demonstrated the initial step of the latter pathway in the reactions of $Cp^*_2ZrH_2$ with other transition-metal carbonyls (eq 1).[4] This reaction type

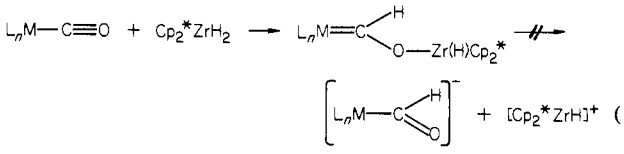

$$L_nM{-}C{\equiv}O + Cp_2^*ZrH_2 \rightarrow L_nM{=}C(H){-}O{-}Zr(H)Cp_2^* \not\rightarrow [L_nM{-}C(H){=}O]^- + [Cp_2^*ZrH]^+ \quad (1)$$

is not unlike the well-known reduction of transition-metal carbonyls with borohydride reagents[5] which, however, afford the formyl anion instead of the corresponding carbene, presumably due to the lower Lewis acidity of the neutral, coordinatively more tolerant trialkylboron vis-à-vis $[Cp^*_2ZrH]^+$ (eq 2).

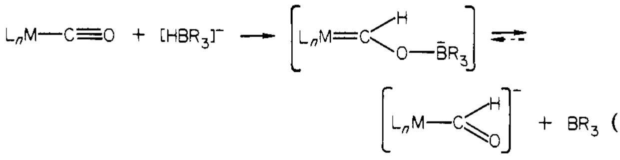

$$L_nM{-}C{\equiv}O + [HBR_3]^- \rightarrow [L_nM{=}C(H){-}O{-}\bar{B}R_3] \rightleftarrows [L_nM{-}C(H){=}O]^- + BR_3 \quad (2)$$

The formation of zirconoxy carbene complexes from $Cp^*_2ZrH_2$ and transition-metal carbonyl hydrides and alkyls presents a particularly interesting possibility, since the resulting species might be expected to rearrange via migratory insertion of carbene into a metal hydride or alkyl bond (Scheme II).[6] Indeed we have found that zirconoxy carbene complexes derived from niobocene carbonyl hydride, $Cp_2Nb(H)(CO)$ ($Cp = \eta^5\text{-}C_5H_5$) and several alkyl and aryl analogues, $Cp_2Nb(R)(CO)$ (R = methyl, benzyl, *p*-methoxybenzyl, vinyl, and phenyl), are stable, isolable compounds. We report herein our studies of the kinetics and mechanism of the migration of the hydride and alkyl substituents to the carbene.

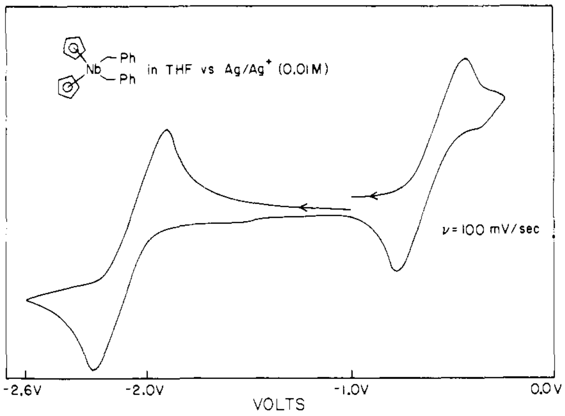

Figure 1. Cyclic voltammogram of $Cp_2Nb(CH_2Ph)_2$ to yield $Cp_2Nb(CH_2Ph)_2^+$ (anodic) and $Cp_2Nb(CH_2Ph)_2^-$ (cathodic) in 1 M Bu_4NBF_4 at Pt wire electrode.

Scheme III

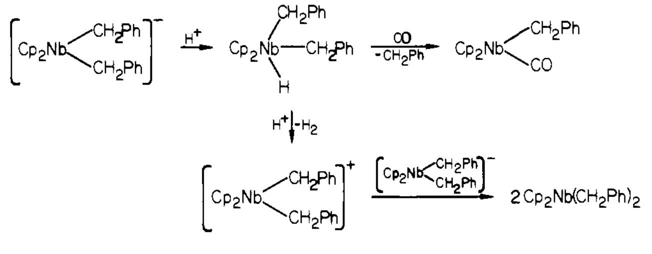

Results

(1) Syntheses of Alkyl- and Aryl-Substituted Niobocene Carbonyls. For the assessment of the relative migratory aptitudes of zirconoxy carbenes with a range of alkyl substituents, the corresponding niobocene carbonyl derivatives were required (vide infra). Only $Cp_2Nb(H)CO$,[7] $Cp_2Nb(CH_3)CO$,[8] and $Cp_2Nb(C(CH_3){=}CH(CH_3))CO$[9] had been reported. In the case of $Cp_2Nb(CH_3)CO$, the literature preparation was not reproducible in our hands. Methyllithium and $Cp_2Nb(Cl)CO$ failed to yield $Cp_2Nb(CH_3)CO$ under all conditions examined. $Cp_2Nb(CH_3)CO$ is obtained in 40% yield, however, by slow addition of CH_3MgBr to $Cp_2Nb(Cl)CO$. Unfortunately, the reactions of both C_6H_5MgBr and $C_6H_5CH_2MgCl$ with $Cp_2Nb(Cl)CO$ failed to yield a significant amount of the desired carbonyl under similar conditions. $Cp_2Nb(C_6H_5)CO$ was successfully obtained by reduction of $Cp_2Nb(C_6H_5)Cl$, prepared via treatment of Cp_2NbCl_2 with 1 equiv of C_6H_5MgBr, with Na/Hg under CO (1 atm) (eq 3). The same

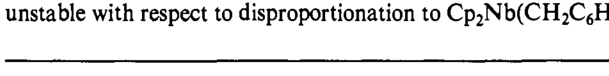

$$Cp_2NbCl_2 + C_6H_5MgBr \rightarrow Cp_2Nb(C_6H_5)(Cl) \xrightarrow[Na/Hg]{CO} Cp_2Nb(C_6H_5)(CO) \quad (3)$$

synthetic route to the benzyl carbonyl derivative fails to yield $Cp_2Nb(CH_2C_6H_5)CO$, since $Cp_2Nb(CH_2C_6H_5)Cl$ appears to be unstable with respect to disproportionation to $Cp_2Nb(CH_2C_6H_5)_2$

---

[4] Wolczanski, P. T.; Threlkel, R. S.; Bercaw, J. E. *J. Am. Chem. Soc.* **1979**, *101*, 218.

[5] (a) Casey, C. P.; Andrews, M. A.; Rinz, J. E. *J. Am. Chem. Soc.* **1979**, *101*, 741. (b) Casey, C. P.; Newman, S. M. *Ibid.* **1978**, *100*, 2554. (c) Tam, W.; Wong, W. K.; Gladysz, J. A. *Ibid.* **1979**, *101*, 1589.

[6] (a) Mango, F. D.; Dvoretzky, I. *J. Am. Chem. Soc.* **1966**, *88*, 2654. (b) Empsall, H. D.; Hyde, E. M.; Markham, M.; McDonald, W. S.; Norton, M. C.; Shaw, B. L.; Weeks, B. *J. Chem. Soc., Chem. Commun.* **1977**, *589*.

[7] Tebbe, F. N.; Parshall, G. W. *J. Am. Chem. Soc.* **1971**, *93*, 3793.

[8] Fredericks, S. J.; Thomas, J. L. *J. Am. Chem. Soc.* **1978**, *100*, 3078.

[9] Labinger, J. A.; Schwartz, J. *J. Am. Chem. Soc.* **1975**, *97*, 1596.

and Cp_2NbCl_2. In agreement with this hypothesis, treatment of Cp_2NbCl_2 with 1 equiv of $C_6H_5CH_2MgCl$ affords only a 50:50 mixture of Cp_2NbCl_2 and $Cp_2Nb(CH_2C_6H_5)_2$. A scheme similar to the preparation of $Cp_2W(CH_2C_6H_5)_2$ from Cp_2WH_2 also fails.[10] Thus deprotonation of $Cp_2Nb(H)CO$ by lithium diisopropyl amide in toluene or diethyl ether followed by reaction with benzyl bromide yields no detectable $Cp_2Nb(CH_2C_6H_5)CO$.

A successful synthesis of $Cp_2Nb(CH_2C_6H_5)CO$ was developed as follows: the reduction of $Cp_2Nb(CH_2C_6H_5)_2$ with Na/Hg followed by protonation of the resulting anion $Cp_2Nb(CH_2C_6H_5)_2^-$ under CO by using CF_3CH_2OH yields $Cp_2Nb(CH_2C_6H_5)CO$ in 60% yield. The cyclic voltammogram of $Cp_2Nb(CH_2C_6H_5)_2$ shows the 17-electron complex has reversible redox potentials of equal intensity at -2.08 V and -0.62 V relative to a Ag/Ag^+ reference electrode (Figure 1). Coulometry of the most cathodic process indicates the reduction is a one-electron transfer to form the 18-electron anion $Cp_2Nb(CH_2C_6H_5)_2^-$. Dilute conditions are required in the protonation with CF_3CH_2OH. A major byproduct, $Cp_2Nb(CH_2C_6H_5)_2$, is taken to indicate that a competing protonation of the intermediate hydride, $Cp_2Nb(CH_2C_6H_5)_2H$, forms $Cp_2Nb(CH_2C_6H_5)_2^+$ and H_2. Subsequent electron transfer from $Cp_2Nb(CH_2C_6H_5)_2^-$ to the cation $Cp_2Nb(CH_2C_6H_5)_2^+$ to yield $Cp_2Nb(CH_2C_6H_5)_2$ (Scheme III) is indeed favorable by 1.46 V, as indicated by cyclic voltammetry.

(2) Preparation of Zirconoxy Carbenes of Niobocene Hydride, Alkyls and Aryls. $Cp^*_2ZrH_2$ (**1**) reacts rapidly with $Cp_2Nb(H)CO$ (**6**) in toluene solution at -78 °C to form $Cp_2(H)Nb{=}CHOZr(H)Cp^*_2$ (**7**) which may be isolated as an orange powder. The ^1H NMR spectrum of **7** is similar to that of the nearly isostructural $Cp_2W{=}CHOZr(H)Cp^*_2$.[4] Thus the resonance of the carbene hydrogen is found at low field (δ 11.63). The resonance due to the cyclopentadienyl hydrogens is a singlet at 25 °C but separates below -35 °C into the expected two singlets of equal intensity separated by only 0.01 ppm. π bonding of the niobium frontier orbitals in the metallocene equatorial plane with the carbene p orbital locks the carbene moiety with its oxygen toward one Cp and hydrogen toward the other Cp for the static structure of **7**.[11] The zirconium hydride and niobium hydride signals are at δ 5.70 and -3.14, respectively.

$Cp_2(H)Nb{=}CHOZr(H)Cp^*_2$ also exhibits temperature-dependent ^{13}C NMR spectra. At 30 °C the resonance due to the carbene is a broad doublet ($^1J_{C-H}$ = 125 Hz) at δ 265.5 which coalesces to a broad signal at -30 °C. At -90 °C, the signal is resolved into two doublets at δ 272.8 ($^1J_{C-H}$ = 139 Hz) and δ 215.1 ($^1J_{C-H}$ = 85 Hz) of approximately 7:1 relative intensity. These data indicate the occurrence of a process which rapidly equilibrates two isomers of $Cp_2(H)Nb{=}CHOZr(H)Cp^*_2$. Models suggest that due to contacts between cyclopentadienyl groups, only two rotomers about the zirconium oxygen bond should be stable conformations. **7a** appears to be the slightly favored rotomer.[12]

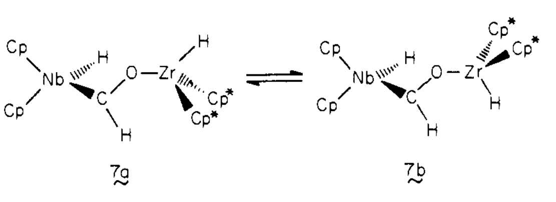

7a **7b**

1 appears to be functioning as a hydride-transfer agent to the carbonyl ligand of **6** (eq 4) as with other metal carbonyls. A reasonable alternate mechanism for the formation of **7** could involve trapping of niobocene formyl by **1** to yield a methylene intermediate (**8**) followed by product forming α-H elimination (eq 5). At -80 °C, $Cp_2(H)Nb{=}CDOZr(D)Cp^*_2$ is the only observed product of the reaction between $Cp^*_2ZrD_2$ and $Cp_2Nb(H)CO$ (eq 6). This result precludes eq 5 or a Lewis acid effect of $Cp^*_2ZrH_2$ in promoting niobium hydride migration to CO and clearly supports the mechanism of eq 4. Furthermore, niobocene alkyl carbonyls react with **1** to yield the corresponding zirconoxy carbenes rather than products which could be associated with alkyl migration to CO (vide infra).

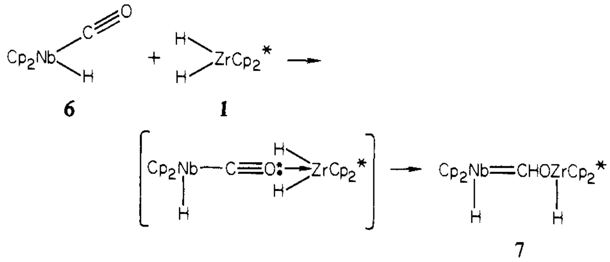

(4)

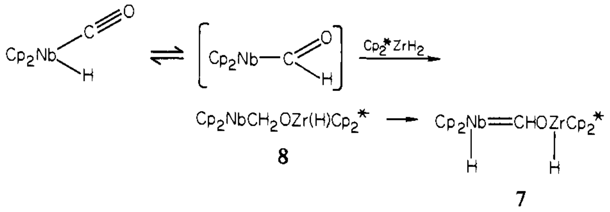

(5)

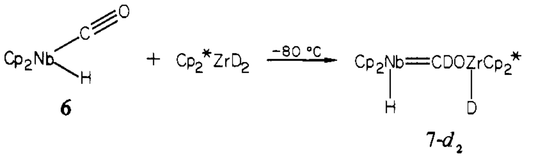

$$\underset{\mathbf{6}}{Cp_2Nb(H)CO} + Cp^*_2ZrD_2 \xrightarrow{-80\ ^\circ C} \underset{\mathbf{7}\text{-}d_2}{Cp_2(H)Nb{=}CDOZr(D)Cp^*_2} \tag{6}$$

The reaction of $Cp^*_2ZrH_2$ with $Cp_2Nb(CH_2Ph)CO$ at -80 °C in toluene solution produces $Cp_2(PhCH_2)Nb{=}CHOZr(H)Cp^*_2$ (**9**), which may be isolated as an orange solid in greater than 90% yield. Below 40 °C, the cyclopentadienyl hydrogens exhibit separate resonances in the NMR spectra, although the difference in chemical shift amounts to only 0.02 ppm. At higher temperatures, these coalesce to a single signal, possibly due to rotation about the niobium–carbene double bond analogous to that observed for the isoelectronic tantalum alkyl/alkylidene complexes.[13]

A variety of substituted niobocene carbenes have been prepared according to eq 7 including those with methyl, phenyl, benzyl, and ($CH_2OZr(H)Cp^*_2$) substituents on niobium. The zirconoxy carbene complex $Cp_2(Cl)Nb{=}CHOZr(H)Cp^*_2$ could not be successfully prepared from **1** and $Cp_2Nb(Cl)CO$, however. In addition to hydride transfer to the carbonyl of $Cp_2Nb(Cl)CO$, **1** also apparently exchanges its hydride ligands with the niobium chloride substituent to form $Cp_2Nb(H)CO$ and $Cp^*_2Zr(H)Cl$. Consistent with this proposal, a mixture of products is obtained in the reaction of $Cp^*_2ZrH_2$ with $Cp_2Nb(Cl)CO$ (NMR). $Cp^*_2Zr(H)Cl$ also will transfer hydride to $Cp_2Nb(H)CO$ as verified independently (eq 8). Due to these complications, no attempt was made to isolate $Cp_2(Cl)Nb{=}CHOZr(H)Cp^*_2$. $Cp_2Zr(H)F$ reacts similarly. $Cp^*_2Zr(H)Cl$ and $Cp^*_2Zr(H)F$ do

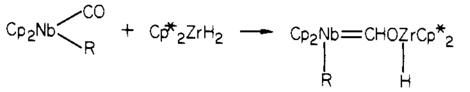

$$Cp_2Nb(R)CO + Cp^*_2ZrH_2 \longrightarrow Cp_2(R)Nb{=}CHOZr(H)Cp^*_2 \tag{7}$$

9, R = $CH_2C_6H_5$; **11**, R = CH_3; **12**, R = $p\text{-}CH_2C_6H_4OCH_3$; **13**, R = $CH_2OZr(H)Cp^*_2$; **14**, R = C_6H_5

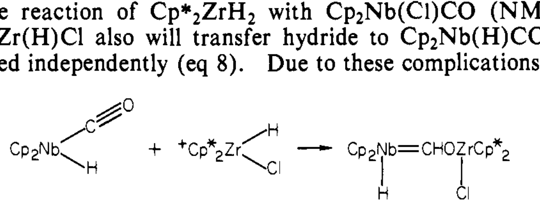

$$Cp_2Nb(H)CO + Cp^*_2Zr(H)Cl \longrightarrow Cp_2(H)Nb{=}CHOZr(Cl)Cp^*_2 \tag{8}$$

---

[10] Francis, B. R.; Green, M. L. H.; Luong-Thi, T.; Moser, G. A. *J. Chem. Soc., Dalton Trans.* **1976**, 1339.

[11] Lauher, J. L.; Hoffmann, R. *J. Am. Chem. Soc.* **1976**, *98*, 1729.

[12] We agree with a reviewer that the large difference in ^{13}C chemical shifts and C-H coupling constants are difficult to reconcile with a conformational change. We see no reasonable alternative explanation of our data, nonetheless.

[13] Guggenberger, L. J.; Schrock, R. R. *J. Am. Chem. Soc.* **1975**, *97*, 6578.

Scheme IV

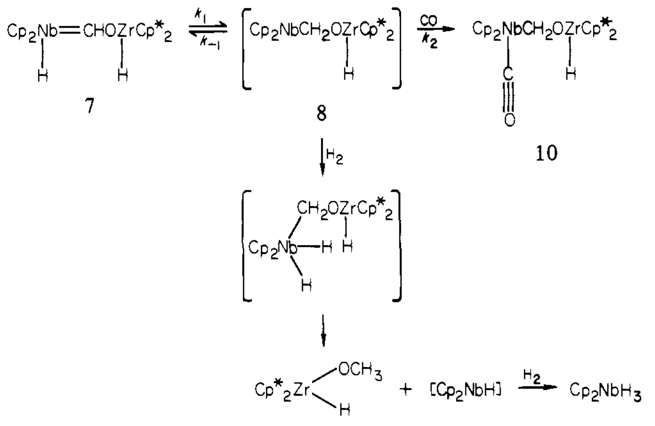

not, however, transfer hydride to the carbonyl ligand of $Cp_2Nb(CH_2Ph)CO$ at 25 °C.

(3) Migratory Insertion of the Zirconoxy Carbene into the Niobocene Hydride Bond. The stability of the 18-electron species $Cp_2(H)Nb{=}CHOZr(H)Cp^*_2$ is perhaps surprising, since this carbene hydride complex is formally the product of α-H abstraction from the tautomer $Cp_2NbCH_2OZr(H)Cp^*_2$. On the other hand, the 16-electron tautomer is expected to be unstable by analogy to the very reactive isoelectronic compounds Cp_2NbH,[7] $Cp_2NbCH_2CH_3$,[14] and $[Cp_2WCH_3]^+$,[15] the last of which has been shown previously to undergo a facile α-H abstraction. This tautomerization (eq 9) can be detected by ^1H NMR spectrometry.

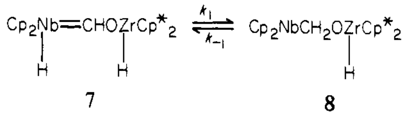

$$\underset{\mathbf{7}}{Cp_2\underset{H}{Nb}{=}CHO\underset{H}{Zr}Cp^*_2} \underset{k_{-1}}{\overset{k_1}{\rightleftharpoons}} \underset{\mathbf{8}}{Cp_2NbCH_2O\underset{H}{Zr}Cp^*_2} \tag{9}$$

Thus at -80 °C, $Cp_2(H)Nb{=}CDOZr(D)Cp^*_2$ displays the spectrum characteristic of **7** lacking the zirconium hydride and carbene–hydrogen resonances. Even at -80 °C however, the niobium hydride signal loses intensity over a period of ca. 15 min concomitant with the appearance of the carbene–hydrogen resonance, indicative of the exchange shown in eq 10. At room

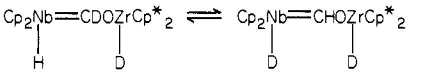

$$Cp_2\underset{H}{Nb}{=}CDO\underset{D}{Zr}Cp^*_2 \rightleftharpoons Cp_2\underset{D}{Nb}{=}CHO\underset{D}{Zr}Cp^*_2 \tag{10}$$

temperature this exchange occurs very rapidly but not so rapidly that the signals for the carbene–hydrogen and the niobium hydride average or significantly broaden on the NMR time scale. This places an upper limit on the exchange rate of $3 \times 10^3\ s^{-1}$.[16]

The availability of this pathway (eq 9) could possibly explain the thermal instability of the niobocene carbene hydride compared to that of the tungsten carbene complex, $Cp_2W{=}CHOZr(H)Cp^*_2$. **7** is unstable above 40 °C whereas $Cp_2W{=}CHOZr(H)Cp^*_2$ is stable for days at 150 °C. Added ligands can, however, trap the reactive, coordinatively unsaturated Nb(III) species. Thus carbon monoxide reacts with the carbene–hydride at 25 °C to form $Cp_2Nb(CO)CH_2OZr(H)Cp^*_2$ (**10**).[4] Hydrogen reacts with **7** at 25 °C to yield equimolar amounts of $Cp^*_2Zr(H)(OCH_3)$ and Cp_2NbH_3.[4] A reasonable mechanism for the latter reaction would involve oxidative addition of H_2 to the coordinatively unsaturated Nb(III) tautomer, reductive elimination of $Cp^*_2Zr(H)(OCH_3)$, and addition of H_2 to the resultant Cp_2NbH yielding Cp_2NbH_3 (Scheme IV).

The reaction of $Cp_2(H)Nb{=}CHOZr(H)Cp^*_2$ with CO may be conveniently followed by visible spectroscopy, since orange $Cp_2(H)Nb{=}CHOZr(H)Cp^*_2$ is converted to green $Cp_2(CO)NbCH_2OZr(H)Cp^*_2$. The rate is first order in the concentration of **7** and first order in $\tilde{p}_{CO}$ over the CO pressure range of 0.3–5.0 atm. The CO concentration in solution at these pressures varies from 2 to 40 mM[17] as compared to a typical initial concentration of **7** of 16 mM. A limiting CO diffusion rate seems unlikely because the reaction rate was insensitive to the stirring speed. The predicted rate expression based on Scheme IV is

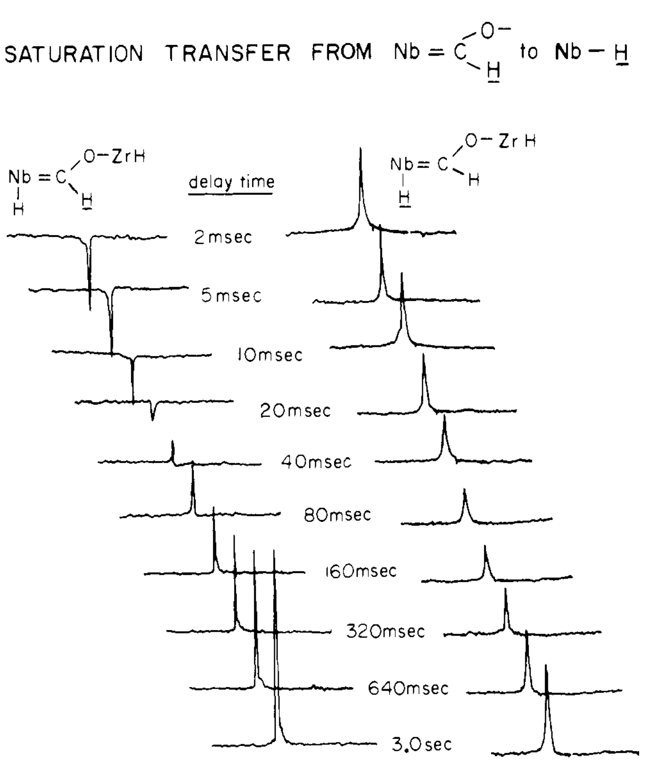

Figure 2. Spin saturation transfer experiments for $Cp_2(H)Nb{=}CHOZr(H)Cp^*_2$ in benzene-d_6 at 32.5 °C. The delay time is the interval between inversion of $Nb{=}C(\mathit{H})O^-$ and the observation pulse.

$$\text{rate} = -\frac{d[\mathbf{7}]}{dt} = \frac{d[\mathbf{10}]}{dt} = k_{obsd}[\mathbf{7}] = \frac{k_1k_2[\mathbf{7}]\tilde{p}_{CO}}{k_{-1} + k_2\tilde{p}_{CO}}$$

$$k_{obsd} = \frac{k_1k_2\tilde{p}_{CO}}{k_{-1} + k_2\tilde{p}_{CO}} \simeq \frac{k_1k_2}{k_{-1}}\tilde{p}_{CO}$$

$$\frac{k_1k_2}{k_{-1}} = 7.6 \times 10^{-3}\ s^{-1}/atm^{-1}$$

Apparently, under these conditions, α-H elimination (k_{-1}) from $Cp_2NbCH_2OZr(H)Cp^*_2$ is much faster than trapping by carbon monoxide ($k_2\tilde{p}_{CO}$).[18] Unfortunately, these measurements of the kinetics of the reaction of **7** with CO provide only the ratio k_1k_2/k_{-1} not the rate constant of interest, k_1.

Since the magnitude of k_1 appeared to preclude the use of NMR line broadening methodology, spin-saturation-transfer methods were attempted to obtain the forward rate for equilibrium 9.[19] This spin-saturation-transfer experiment does indeed yield the value of k_1. A typical experiment involves inverting one signal, then waiting a specified time before recording the spectrum. The exchange rate is obtained by relating the intensities of the inverted peak to the peak due to the exchanging proton as a function of

---

(14) Guggenberger, L. J.; Meakin, P.; Tebbe, F. N. *J. Am. Chem. Soc.* **1974**, *96*, 5420.

(15) (a) Cooper, N. J.; Green, M. L. H. *J. Chem. Soc., Chem. Commun.* **1974**, 208. (b) Copper, N. J.; Green, M. L. H. *Ibid.* **1974**, 761.

(16) Leyden, D. E.; Cox, R. H. "Analytical Applications of NMR"; Wiley: New York, 1977; p 283.

(17) "International Critical Tables"; McGraw-Hill: New York, 1926; Vol. I, p 265.

(18) Whereas it could be argued that H migration is assisted by incoming CO, the measured rate of k_1 (and hence k_{-1}) indicates α-H elimination is much faster than trapping by CO, even at 5 atm. See results of spin saturation transfer experiments.

(19) (a) Forsen, S.; Hoffmann, R. A. *J. Chem. Phys.* **1964**, *40*, 1189. (b) Dahlquist, F. W.; Longmuir, K. J.; DuVernet, R. B. *J. Magn. Reson.* **1975**, *17*, 406.

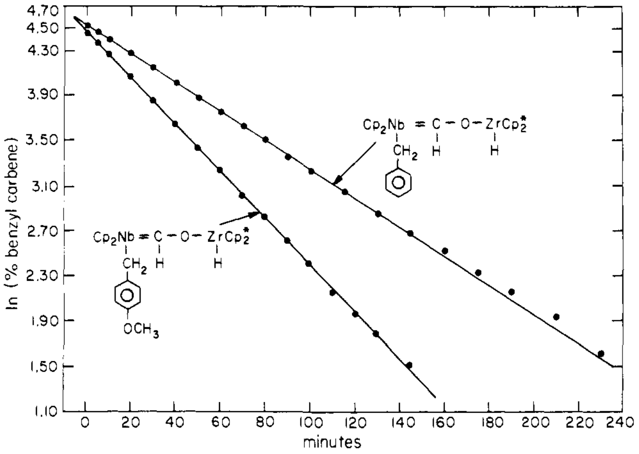

Figure 3. Log or natural log plots of the percentage of **9** and **11** (^{1}H NMR) as a function of time.

delay time from the moment of complete inversion. The correlation of the difference in intensity of the two peaks as a function of delay time with the magnetization equation yields the exchange rate.[20]

Figure 2 shows a series of spectra for the spin saturation transfer of magnetization from the carbene hydrogen to the niobium hydride. The nonlinear least-squares fit of the series of spectra to the magnetization equation yields a rate of exchange equal to 15.7 s^{-1} at 32.5 °C. The measured rate is identical when either the niobium hydride or the carbene hydrogen resonance is saturated. Since either methylene proton can α-H eliminate from $Cp_2NbCH_2OZr(H)Cp^*_2$, the insertion rate at 32.5 °C equals 31.4 s^{-1}, twice the exchange rate. The rate is observed to be invariant over a fourfold concentration range of **7**, indicating that the hydride migration is unimolecular. These results in conjunction with the results of kinetic measurements show that α-H elimination is roughly 4100 times faster than CO trapping at 1 atm.[18] Exchange rates were measured from 10 °C to near the decomposition temperature of **7** (40 °C). An Arrhenius plot at four temperatures yields the activation parameters $\Delta H^{\ddagger} = 13.1 \pm 1.4$ kcal mol^{-1} and $\Delta S^{\ddagger} = -9.6 \pm 2.3$ eu (Table I).

(4) Migratory Insertion of the Zirconoxy Carbene into Niobocene Alkyl Bonds. The alkyl-substituted niobocene carbenes of the general formula $Cp_2(CH_2R)Nb{=}CHOZr(H)Cp^*_2$ afford *trans*-$Cp^*_2Zr(H)(OCH{=}CHR)$ and $Cp_2Nb(H)(PhC{\equiv}CPh)$ or Cp_2NbH_3 in the presence of diphenylacetylene or dihydrogen, respectively (eq 11 and 12). A plausible reaction sequence leading

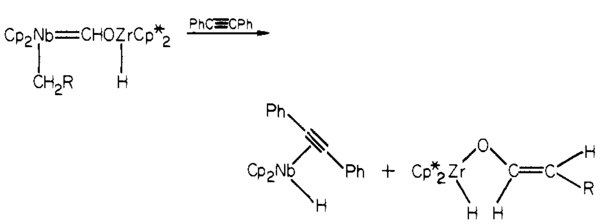

(11)

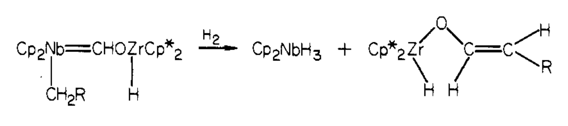

(12)

to these products would involve insertion of the zirconoxy carbene into the niobium alkyl bond followed by rapid β-H elimination to yield the *trans*-zirconium enolate and Cp_2NbH, which is trapped by $PhC{\equiv}CPh$ or H_2. When CO is the promoting ligand, a secondary reaction is also observed. The initial products, $Cp_2Nb(H)(CO)$ and *trans*-$Cp^*_2Zr(H)(OCH{=}CHPh)$ react further to yield what appears by NMR spectrometry to be $Cp_2(CO)NbCH_2OZr(OCH{=}CHPh)Cp^*_2$ via a subsequent hydride transfer analogous to that between $Cp^*_2Zr(H)(Cl)$ and $Cp_2Nb(H)(CO)$ (eq 13).

Table I. Exchange Rates for the Tautomerization of **7** (eq 9) Obtained via Spin Saturation Transfer Experiments

T, °C	[**7**], mM	resonance inverted	T_1, average proton relaxation time, s	k_{ex}, s^{-1}
10	51	Nb=C*H*-	0.525	3.3 ± 0.4
20	51	Nb=C*H*-	0.625	7.6 ± 0.4
32.5	51	Nb=C*H*-	0.835	15.2 ± 0.9
42	51	Nb=C*H*-	0.935	40.5 ± 2.4
32.5	51	Nb-*H*	0.835	15.7 ± 0.8
32.5	200	Nb=C*H*-	0.67	14.5 ± 0.9

Table II. Kinetic Data for Migratory Insertion Reactions of $Cp_2(CH_2R)Nb{=}CHOZr(H)Cp_2^*$ with $PhC{\equiv}CPh$ (50 °C, Benzene-d_6)

compd	10^4k_{obsd}, s^{-1}	notes
$Cp_2(PhCH_2)Nb{=}CHOZr(H)Cp^*_2$	2.08 (1)	yield > 95% (^{1}H NMR)
$Cp_2(PhCD_2)Nb{=}CHOZr(H)Cp^*_2$ (**9**-d_2)	1.82 (2)	only $Cp_2^*Zr(H)(OCH{=}CDPh)$ is formed
$Cp_2(PhCH_2)Nb{=}CDOZr(D)(Cp^*\text{-}d_{15})_2$- (**9**-$d_2$)	2.59 (4)	only $(Cp^*\text{-}d_{15})_2Zr(D)(OCD{=}CHPh)$ is formed
$Cp_2(CH_3)Nb{=}CHOZr(H)Cp^*_2$	7.64 (6)	k_{obsd} is that for disappearance of **10**; yield ≃87%
$Cp_2(p\text{-}CH_3OC_6H_4CH_2)Nb{=}CHOZr(H)Cp^*_2$ (**12**)	3.25 (3)	yield > 95% (^{1}H NMR)
$Cp_2(Cp^*_2(H)ZrOCH_2)Nb{=}CHOZr(H)Cp^*_2$ (**13**)	3.33 (5)	yield of *trans*-$[Cp^*_2Zr(H)]_2(\mu\text{-}OCH{=}CHO)$ > 95% (^{1}H NMR); ref 3a

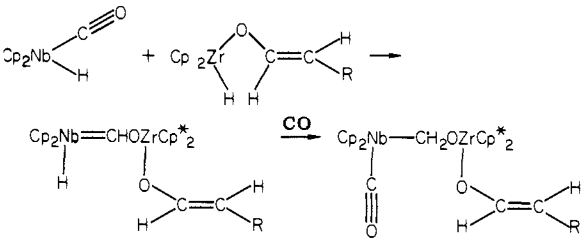

(13)

With use of ^{1}H NMR spectrometry to monitor the reactions, kinetic data (Figure 3) were obtained at 50 °C with $PhC{\equiv}CPh$ as the trapping ligand (eq 11). In all cases, the reaction rate is first order in $[Cp_2(CH_2R)Nb{=}CHOZr(H)Cp^*_2]$ for 3–5 half-lives and independent of $[PhC{\equiv}CPh]$ over the concentration range 2.4–120 mM. The kinetic data are summarized in Table II. The isotope effect for the deuterium-substituted benzylic carbene $Cp_2(CD_2Ph)Nb{=}CHOZr(H)Cp^*_2$ is 1.17. An inverse isotope effect is observed in the deuterium-labeled carbene $Cp_2(CH_2Ph)Nb{=}CDOZr(D)Cp^*_2$: $k_H/k_D = 0.79$. The reaction rates for **9** and **10** were monitored at several temperatures between 32.5 and 80 °C. The activation parameters obtained from the least-squares fits to the Arrhenius plots (Figure 4) are $\Delta H^{\ddagger} = 25.7 \pm 0.7$ kcal mol^{-1} and $\Delta S^{\ddagger} = 3.8 \pm 1.3$ eu for the benzyl migration and $\Delta H^{\ddagger} = 23.2 \pm 1.7$ kcal mol^{-1} and $\Delta S^{\ddagger} = -0.9 \pm 2$ eu for the methyl migration.

(5) Reactivity of $Cp_2(Ph)Nb{=}CHOZr(H)Cp^*_2$. Unlike the carbene alkyls, $Cp_2(Ph)Nb{=}CHOZr(H)Cp^*_2$ (**14**) does not react readily with CO. Only slow decomposition occurs when **14** is warmed above 80 °C under CO. A reaction is observed under 2 atm of H_2 at 70 °C; however, the products have not been fully

---

[20] Kooistra, D. A.; Richards, J. H.; Smallcombe, S. H. *Org. Magn. Reson.* **1980**, *13*, 1.

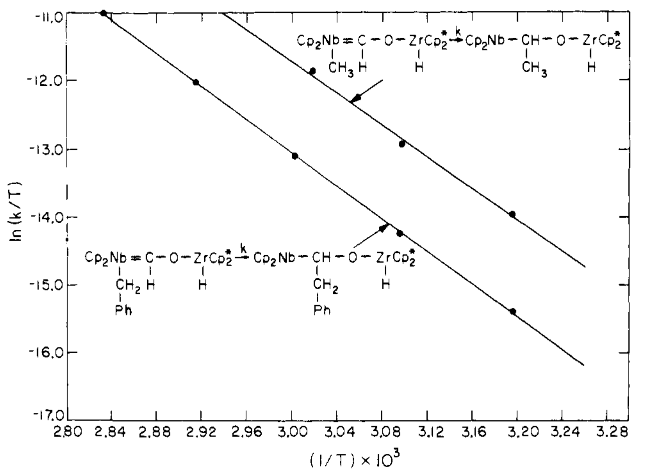

Figure 4. Arrhenius plots for the migratory insertion reactions of $\mathrm{Cp_2(CH_3)Nb{=}CHOZr(H)Cp^*_2}$ and $\mathrm{Cp_2(PhCH_2)Nb{=}CHOZr(H)Cp^*_2}$ promoted by $\mathrm{PhC{\equiv}CPh}$.

Scheme V

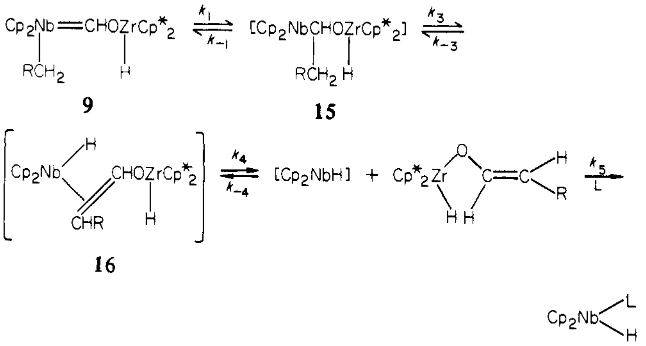

characterized. The reactions of **14** are presently under investigation and will be reported in a forthcoming publication.

Discussion

A series of compounds which allow for a systematic study of carbene insertion reactions has been obtained via the apparently general reaction (eq 7). The relative migratory aptitudes of

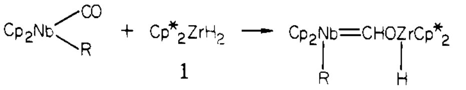

$$\underset{\mathbf{1}}{\mathrm{Cp_2Nb(CO)R}} + \mathrm{Cp^*_2ZrH_2} \longrightarrow \mathrm{Cp_2Nb(R){=}CHOZr(H)Cp^*_2} \qquad (7)$$

R = H, alkyl, aryl, etc.

hydride, alkyl, and aryl are of special interest. These are directly related to the rate constant(s) k_1 (and k_{-1}) (eq 14). In the case

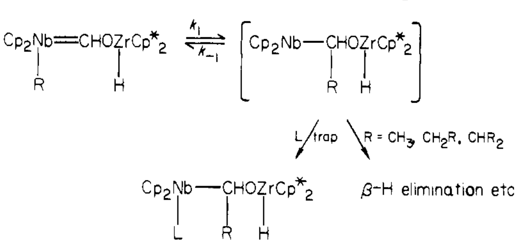

$$\mathrm{Cp_2Nb(R){=}CHOZr(H)Cp^*_2} \underset{k_{-1}}{\overset{k_1}{\rightleftharpoons}} \left[\mathrm{Cp_2Nb{-}CH(R)OZr(H)Cp^*_2}\right] \xrightarrow{\mathrm{L/trap}} \mathrm{Cp_2Nb(L){-}CH(R)OZr(H)Cp^*_2}$$

$$\xrightarrow{\mathrm{R\,=\,CH_3,\ CH_2R,\ CHR_2}} \beta\text{-H elimination etc} \qquad (14)$$

of $\mathrm{Cp_2(H)Nb{=}CHOZr(H)Cp^*_2}$ (**7**), the spin-saturation-transfer experiments provide the value for k_1 directly. The rates of alkyl migration (k_1) for **9**, **11**, **12**, and **13** are not immediately obvious from the kinetic data of Table II, since several subsequent steps are involved in the overall transformation to the zirconium enolate products (Scheme V). The following results do, however, support a rate-limiting intramolecular migratory insertion (k_1 step) for **9** and also for **11**, **12**, and **13**. (i) No detectable concentrations of any intermediates such as **15** or **16** are observed during the reaction. (ii) The overall rate is independent of the concentration of trapping ligand ($\mathrm{PhC{\equiv}CPh}$). (iii) **9**-d_2, the benzylic isotopomer (Table II), exhibits a normal secondary deuterium kinetic isotope effect ($k_H/k_D = 1.17$), whereas (iv) **9**-d'_2, the carbene/zirconium isotopomer (Table II), exhibits an inverse deuterium kinetic isotope effect ($k_H/k_D = 0.79$). (v) A crossover experiment indicates no significant homolysis of the niobium benzyl bond occurs during the reaction: a 1:1 mixture of $\mathrm{Cp_2(CD_2Ph)Nb{=}CHOZr(H)Cp^*_2}$ and $\mathrm{Cp_2(CH_2Ph)Nb{=}CDOZr(D)(Cp^*\text{-}d_{15})_2}$ produces no detectable $\mathrm{Cp^*_2Zr(H)(OCH{=}CHPh)}$. Observations i and ii eliminate the ligand-trapping step (k_5) as rate-limiting, leaving only two possible situations: a fast preequilibrium between **9** and **15** followed by rate-limiting β-H elimination (k_3) or rate-limiting migratory insertion (k_1). Observation iii could be taken as consistent with either possibility, but iv is most consistent with a rate-limiting k_1 step. An inverse deuterium isotope effect of this magnitude has been taken to indicate a net increase in p character of the deuterium substituted carbon in the transition state.[21] Thus, rate-limiting migratory insertion (sp^2 carbene → sp^3 methine) rather than β-H elimination (sp^3 methine → sp^2 olefin) is most consistent with the observed inverse isotope effect. The former possibility seems unlikely in any case since a fast equilibrium between **9** and **15** would require that the rate of α-benzylic abstraction exceed the rates of both α-H abstraction (cf. the rapid tautomerization of **7**) and the normally facile β-H elimination,[22] a seemingly untenable requirement. Thus the measured rates for the reaction **11** listed in Table II do indeed reflect the relative migratory aptitudes of the alkyl groups of **9**, **11**, **12**, and **13** for comparison to that for the hydride ligand of **7**.

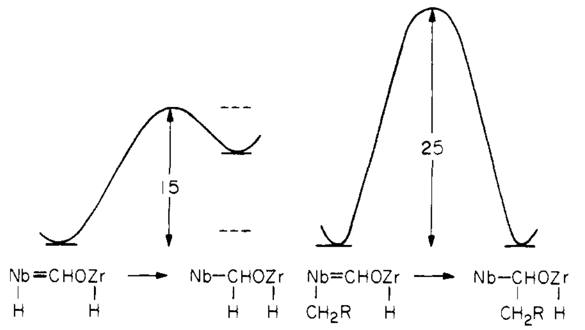

Figure 5. Partial free-energy surfaces for hydride and alkyl migration to zirconoxy carbene derivatives of niobocene.

This series of migratory aptitudes, H ≫ $\mathrm{CH_3}$ > $\mathrm{CH_2Ph}$, could be attributed to the relative thermodynamics of the migratory insertion step. The free-energy change of the elementary step (eq 9) can be bracketed, considering the measured activation energy

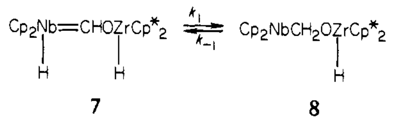

$$\underset{\mathbf{7}}{\mathrm{Cp_2Nb(H){=}CHOZr(H)Cp^*_2}} \underset{k_{-1}}{\overset{k_1}{\rightleftharpoons}} \underset{\mathbf{8}}{\mathrm{Cp_2NbCH_2OZr(H)Cp^*_2}} \qquad (9)$$

$3 < \Delta G < 15$ kcal mol^{-1}

and absence of detectable equilibrium amounts of the methylene tautomer **8** in solutions of **7** (^{1}H NMR). The migratory insertion reactions of the niobium alkyls do not involve preequilibria (vide supra), so that it is not possible to accurately bracket the free-energy change for these cases (eq 15). A rough estimate of

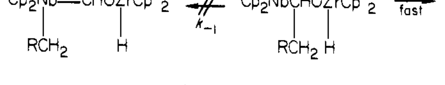

$$\mathrm{Cp_2Nb(RCH_2){=}CHOZr(H)Cp^*_2} \underset{k_{-1}}{\overset{k_1}{\not\rightleftharpoons}} \mathrm{Cp_2NbCH(RCH_2)OZr(H)Cp^*_2} \xrightarrow[\text{fast}]{k_3} \qquad (15)$$

relative free energy changes for eq 9 and 15 can be made, however, by comparing relative bond energies: Nb–H vs. $\mathrm{Nb{-}CH_2R}$ and C–H vs. $\mathrm{C{-}CH_2R}$. The limited data available indicate that

---

(21) (a) Alder, R. W.; Baker, R.; Brown, J. M. "Mechanism in Organic Chemistry"; Wiley-Interscience: New York, 1971; p 19. (b) Brown, P.; Cookson, R. C. *Tetrahedron* **1965**, *21*, 1993.

(22) Kochi, J. K. "Organometallic Mechanisms and Catalysis"; Academic Press: New York, 1978; p 246.

Table III. Analytical and NMR Data (Benzene-d_6)

compd	group	chem shift, δ
$(C_5H_5)_2(H)Nb{=}CHOZr(H)(C_5Me_5)_2$ (7) (toluene-d_8, −35 °C)	C_5H_5, s	5.01
Anal. Calcd: C, 60.46; H, 7.04	C_5H_5, s	5.02
Found: C, 58.76; H, 6.80	Nb–H, s	−3.14
	=CH–O–, s	11.63
	ZrH, s	5.70
	$C_5(CH_3)_5$, s	1.99
$(C_5H_5)_2(CH_3)Nb{=}CHOZr(H)(C_5Me_5)_2$ (11)	C_5H_5, s	4.97
Anal. Calcd: C, 61.02; H, 7.20; Zr, 14.48	$C_5H'_5$, s	5.01
Found: C, 60.85; H, 7.10; Zr, 14.21	Nb–CH_3, s	0.00
	=CH–O–, s	11.72
	Zr–H, s	5.90
	$C_5(CH_3)_5$, s	1.95
	$C_5(CH_3)_5$, s	1.97
$(C_5H_5)_2(PhCH_2)Nb{=}CHOZr(H)(C_5Me_5)_2$ (9)	C_5H_5, s	4.98
Anal. Calcd: C, 64.65; H, 7.00; Zr, 12.92; Nb, 13.16	$C_5H'_5$, s	4.96
Found: C, 61.64; H, 6.56; Zr, 12.48; Nb, 12.85	Nb–C*H*H'Ph, d	2.73 ($^3J_{HH'}$ = 11 Hz)
	Nb–CHH'Ph, d	1.99
	=CH–O–, s	11.87
	Zr–H, s	6.05
	$C_5(CH_3)_5$, s	1.96
	$C_5(CH_3)_5$, s	2.03
	C_6H_5, m	7.28
$(C_5H_5)_2(CH_2Ph)Nb{=}CDOZr(D)(C_5(CD_3)_5)_2$	C_5H_5, s	4.98
	$C_5H'_5$, s	4.96
	Nb–C*H*HPh, d	2.73 ($^3J_{HH}$ = 11 Hz)
	Nb–CH*H*Ph, d	1.99
	C_6H_5, m	7.28
$(C_5H_5)_2(CH_3OC_6H_4CH_2)Nb{=}CHOZr(H)(C_5Me_5)_2$ (12)	C_5H_5, s	4.99
Anal. Calcd: C, 63.65; H, 6.98	Nb–C*H*H'–, d	2.68 ($^3J_{HH}$ = 11 Hz)
Found: C, 61.53; H, 6.81	Nb–CH*H'*–, d	2.00
	Nb=CH-O–, s	11.76
	$C_6\mathit{H}_2H'_2$, d	6.87 ($^3J_{HH}$ = 8 Hz)
	$C_6H_2\mathit{H}'_2$, d	7.70
	OCH_3, s	3.45
	Zr–H, s	6.02
	$C_5(CH_3)_5$, s	1.93, 2.02
$(C_5H_5)_2(C_6H_5)Nb{=}CHOZr(H)(C_5Me_5)_2$ (14)	C_5H_5, s	5.14
Anal. Calcd: C, 64.23; H, 6.85; Zr, 13.18; Nb, 13.43	$C_5H'_5$, s	5.23
Found: C, 64.19; H, 6.88; Zr, 12.91; Nb, 13.31	Nb–C_6H_5, s	7.2
	Nb=CH–O–, s	12.23
	Zr-H	6.90
	$C_5(C\mathit{H}_3)_5$	2.01
$(C_5H_5)_2((C_5Me_5)_2(H)ZrOCH_2)Nb{=}CHOZr(H)(C_5Me_5)_2$ (13)	C_5H_6, s	5.12
Anal. Calcd: C, 61.99; H, 7.50; Zr, 18.11	$C_5H'_5$, s	5.33
Found: C, 61.85; H, 7.39; Zr, 18.33	Nb–CH_2–O, s	5.93
	ZrH, s	6.10
	ZrH', s	6.65
	$C_5(CH_3)_5$, s	1.94
	s	1.99
	s	2.04
	s	2.10
$(C_5H_5)_2(C_6H_5CH_2)Nb{=}CHOZr(I)(C_5Me_5)_2$	C_5H_5, s	4.97
	C_5H_5, s	5.06
	Nb–CH_2–, d	2.65 ($^3J_{HH}$ = 10 Hz)
	-CH_2–$C_6\mathit{H}_5$, m	7.23
	Nb=CH–O–, s	11.30
	$C_5(CH_3)_5$, s	1.90
	$C_5(CH_3)_5$, s	1.97
$(C_5H_5)_2Nb(CH_2C_6H_5)CO$	C_5H_5, s	4.39
Anal. Calcd: C, 63.17; H, 5.01; Nb, 27.15	Nb–CH_2–, s	1.82
Found: C, 63.04; H, 5.15; Nb, 27.00	CH_2–$C_6\mathit{H}_5$, m	7.23
$(C_5H_5)_2Nb(CH_2C_6H_4OCH_3)CO$	C_5H_5, s	4.40
	Nb–CH_2–, s	1.84
	CH_2–$C_6H_2H_2$–O, d	6.88 ($^3J_{HH}$ = 8 Hz)
	CH_2–$C_6H_2H_2$–O, d	7.17
	OCH_3, s	3.45
$(C_5H_5)_2Nb(C_6H_5)CO$	C_5H_5, s	4.53
Anal. Calcd: C, 62.22; H, 4.61; Nb, 28.31	C_6H_5, m	7.05, 7.70
Found: C, 62.34; H, 4.74; Nb, 28.08		
$(C_5H_5)_2Nb(CO)CH_2OZr(H)(C_5Me_5)_2$	C_5H_5, s	4.68
Anal. Calcd: C, 59.70; H, 6.58; Zr, 14.17	Nb–CH_2-O–, s	5.20
Found: C, 59.36; H, 6.94; Zr, 14.33	$NbC^{13}H_2$-O–, d	5.20 ($J_{C^{13}H}$ = 138 Hz)
	ZrH, s	5.20
	$C_5(CH_3)_5$, s	2.00
$(C_5H_5)_2Nb(H)[(C_6H_5)_2C_2]$	C_5H_5, s	4.85
Anal. Calcd: C, 71.64; H, 5.26; Nb, 23.09	Nb–H, s	−0.28
Found: C, 71.67; H, 5.37; Nb, 23.05	-C_6H_5, m	7.5

Table III (*Continued*)

compd	group	chem shift, δ
$(C_5Me_5)_2Zr(H)(OCH{=}CHPh)$, trans	$C_5(CH_3)_5$, s	1.93
Anal. Calcd: C, 69.80; H, 7.95	ZrH, s	6.23
Found: C, 70.80; H, 7.55	-O–CH=, d	5.73 $^3J_{HH}$ = 12 Hz)
	=CHPh, d	7.52
	$-C_6H_5$, m	7.08
$(C_5Me_5)_2Zr(H)(OCH{=}CHPh)$, cis	$C_5(CH_3)_5$, s	1.88
	ZrH, s	6.43
	-OCH=, d	6.69 ($^3J_{HH'}$ = 7 Hz)
	=CHPh, d	5.10
	$-C_6H_5$, m	7.08
$(C_5Me_5)_2Zr(H)(OCH{=}CH_2)$	$C_5(CH_3)_5$, s	1.92
	ZrH, s	6.10
	O–CH=, dd	6.77
	$=CH_2$ (t), d	4.10 ($^3J_{HH'}$ = 17 Hz)
	$=CH_2$ (c), d	3.89 ($^3J_{HH'}$ = 5 Hz)

transition metal–hydride bond energies are approximately 25 kcal mol^{-1} stronger than the corresponding transition metal–alkyl bond strengths,[23] whereas the average C–H bond energy exceeds the average C–CH$_2$R bond strength by only 15 kcal mol^{-1}.[24] This relationship together with the conclusion concerning the energetics of eq 9 and the measured activation energies for alkyl migration leads to the two partial free-energy surfaces shown in Figure 5. The important conclusion here is that free-energy change for alkyl migration (eq 15) is 10 kcal mol^{-1} more favorable than that for hydride migration or roughly thermoneutral. Thus the relative free energy changes (eq 9 vis-à-vis eq 15) do not reflect the relative migratory aptitudes, since the most endothermic reaction (eq 9) proceeds more than 6 orders of magnitude faster. We conclude, therefore, that the relative rates must depend on some property of the migrating group which influences primarily the transition state.

The large difference in the energy of the transition state for hydride migration (h‡) and that for alkyl migration (c‡) may be reflect the greater stability of three-center, two-electron bonds involving hydrogen, generally attributed to better overlap of a less-directional s valence orbital. Similar arguments have been made to rationalize the relative migratory aptitudes H > aryl > alkyl in Wagner–Meerwien and pinacol rearrangements.[25] Although the differences in the rates of migration among the alkyl groups examined are small, the order (CH$_3$ > CH$_2$Ph) parallels that observed for alkyl migration to carbon monoxide.[26] Furthermore, zirconoxy carbene, like carbon monoxide, appears to function as an electrophile in the migratory insertion.[27] In accord with the electrophilic nature of the inserting carbene, substitution of an electron-donating methoxy group on the benzyl substituent enhances the rate of migration. It is worth noting in this connection that alkylidene complexes of the type Cp$_2$Ta(CHR)(CH$_2$R), shown to react as nucleophiles,[28] fail to undergo migratory insertion.[29] Clearly the oxygen substituent is responsible for this inversion in the polarity of the carbene.[30]

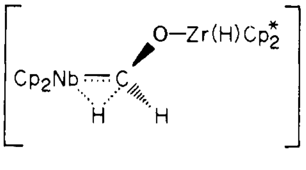

h‡

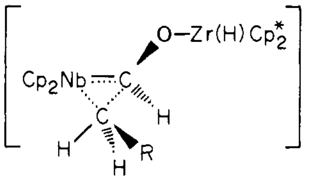

c‡

Scheme VI

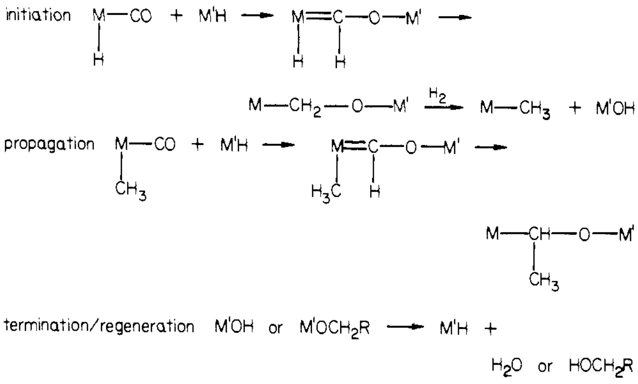

The thermodynamics of the overall migratory insertion rather than transition-state effects can dominate the reactivity of metal carbonyl hydrides, however. Thus the migration of hydride to CO to afford a metal formyl is much more endothermic than the corresponding alkyl migration, at least insofar as the former process has been observed to proceed only in reverse,[31] whereas the alkyl–acyl rearrangement is often facile in both directions.[22,26,32]

The observed rapid hydride transfer to a metal carbonyl, forming an oxycarbene, and the subsequent migratory insertions of carbenes into both metal hydride and metal alkyl bonds suggest a possibly general mechanism for CO hydrogenation to oxygenates, etc. (Scheme VI). Rather than intramolecular hydride migration to CO,[33] the initial hydrogen transfer to CO could occur in a bimolecular step from another metal hydride. The resultant oxycarbene would then be expected to rapidly insert into a hydride bond to form a μ-CH$_2$O species. The attractive feature of this mechanism is that it circumvents the endothermic step involving intramolecular hydride migration to CO. In order to achieve a catalytic CO reduction, it is necessary to hydrogenate the metal alkoxide or metal hydroxide to regenerate the metal hydride. For zirconium alkoxides, the zirconium oxygen bond is probably too robust to allow for zirconium hydride regeneration with hydrogen.[33] This bond strength is undoubtedly one of the driving forces which causes such rapid hydride transfer to the carbonyl ligand of Cp$_2$Nb(H)CO. We are presently investigating the generality

---

[23] (a) Rathke, J. W.; Feder, H. M. *J. Am. Chem. Soc.* **1978,** *100,* 3625. (b) Halpern, J.; Ng, F. T. T.; Runpel, G. L. *Ibid.* **1979,** *101,* 7124. (c) Connor, J. A. *Top. Curr. Chem.* **1977,** *71,* 71.

[24] Benson, S. W. "Thermochemical Kinetics"; Wiley: New York, 1976.

[25] (a) March, J. "Advanced Organic Chemistry"; McGraw-Hill: New York, 1968; p 788. (b) Rocker, Y. "Molecular Rearrangement"; de Mayo, P., Ed.; Interscience: New York, 1963.

[26] (a) Wojcicki, A. *Adv. Organomet. Chem.* **1973,** *11,* 88. (b) Calderazzo, F. *Angew. Chem., Int. Ed. Engl.* **1979,** 229.

[27] (a) Butts, S. B.; Holt, E. M.; Strauss, S. H.; Alcock, W. W.; Stimson, R. E.; Shriver, D. F. *J. Am. Chem. Soc.* **1979,** *101,* 6450. (b) Davison, A.; Martinez, N. *J. Organomet. Chem.* **1974,** *74,* C17.

[28] Schrock, R. R. *J. Am. Chem. Soc.* **1975,** *97,* 6577.

[29] Schrock, R. R.; Sharp, P. R. *J. Am. Chem. Soc.* **1978,** *100,* 2389.

[30] Cardin, D. J.; Cetinkaya, B.; Lappert, M. F. *Chem. Rev.* **1972,** *72,* 545.

[31] Collman, J. P.; Winter, S. R. *J. Am. Chem. Soc.* **1973,** *95,* 4089.

[32] (a) Kubota, M.; Blake, D. M.; Smith, S. A. *Inorg. Chem.* **1971,** *10,* 1430. (b) Cawse, J. N.; Fiato, R. A.; Pruett, R. L. *J. Organomet. Chem.* **1979,** *172,* 405.

[33] (a) Henrici-Olivé, G.; Olivé, S. *Angew. Chem., Int. Ed. Engl.* **1976,** *15,* 136. (b) Keim, W.; Berger, M.; Schlupp, J. *J. Catal.* **1980,** *61,* 359.

of this hydride-transfer reaction with other transition-metal complex hydrides.

Experimental Section

General Considerations. All manipulations were performed in an inert atmosphere by using a nitrogen-filled Vacuum Atmospheres glovebox or using high vacuum techniques. Glyme and THF were distilled from sodium benzophenone ketyl. All other solvents including NMR solvents (benzene-d_6 and toluene-d_6) were purified by vacuum transfer from "titanocene".[35] Hydrogen, argon, and nitrogen were passed through MnO on vermiculite[36] and 4-Å molecular sieves. Carbon monoxide (MCB) was used without purification. Diphenylacetylene was recrystallized from octane. $Cp_2Nb(CO)(H)$,[36] $Cp_2Nb(Cl)CO$,[37] $Cp^*_2ZrH_2$,[38] and Cp_2NbCl_2[39] were prepared by literature methods. $Cp^*_2Zr(H)F$ was prepared from $Cp^*_2ZrH_2$ and $Cp^*_2ZrF_2$ by using a method analogous to that for $Cp^*_2Zr(H)Cl$.[40]

^1H NMR spectra were obtained by using either a Varian EM 390 or a JEOL FX90Q spectrometer. ^{13}C NMR spectra were also measured on the JEOL instrument. Infrared spectra were recorded on a Beckman 4240 spectrophotometer. ESR spectra were obtained on an X-band Varian E-line Century Series spectrometer. Visible spectra were observed by using a Cary 14 spectrophotometer. Cyclic voltammetry was conducted on a PAR 174 A Polarographic analyzer. Coulometry was analyzed with a PAR Potentiostat 173. Elemental analyses were obtained from Bernhardt or from Caltech analytical laboratories.

Preparation of $Cp_2Nb(CH_3)(CO)$. A 2.0-g sample of $Cp_2Nb(Cl)CO$ (7.0 mmol) was suspended in 140 mL of toluene at 45 °C. A 2.0-mL sample of 3.2 M methylmagnesium bromide (6.4 mmol) (Aldrich) was added in the following manner: 10% was added at once followed by the slow addition of the remainder over a period of 15 min. The toluene was immediately removed by vacuum transfer. Several pentane extractions, followed by treatment with methyl iodide, yielded a green solid after solvent removal. The green residue was extracted with pentane to separate $Cp_2Nb(CH_3)CO$ from $Cp_2Nb(I)CO$. Sublimation (75 °C (10^{-3} torr)) yielded 0.8 g of $Cp_2Nb(CH_3)CO$, 43% yield.

Preparation of $Cp_2Nb(Ph)(CO)$. A 2.0-g sample of Cp_2NbCl_2 (6.8 mmol) was treated with 2.1 mL of 3.2 M phenylmagnesium bromide (6.7 mmol) (Aldrich) in 50 mL of THF at 25 °C. After 8 h, all the Cp_2NbCl_2 had dissolved and a brown solution and considerable white precipitate remained. All solvent was removed by vacuum transfer. The resulting brown solid was extracted with 70 mL of warm toluene, followed by solvent removal which left green-brown crystals, presumably of $Cp_2Nb(Ph)(Cl)$. After this intermediate was redissolved in toluene and cooled to −80 °C, 4 mL of 1% Na/Hg was added via syringe. All gas was removed and replaced with 1 atm of CO and the reaction mixture was stirred at 25 °C for 8 h. The resulting green solution was decanted from the amalgam and filtered prior to solvent removal. The green solid was sublimed at 120 °C and 10^{-3} torr to yield 0.9 g of $Cp_2Nb(Ph)CO$, 40% based on Cp_2NbCl_2.

Preparation and Characterization of $Cp_2Nb(CH_2C_6H_4X)_2$ (X = H and OCH_3). A 2.0-g sample of Cp_2NbCl_2 (6.8 mmol) was suspended in 100 mL of THF. A 17-mL sample of 0.92 M benzylmagnesium chloride (15.6 mmol) was added and the reaction stirred for 6 h. The excess Grignard in the resultant purple solution was quenched with 1 mL of deoxygenated methanol. All solvent was immediately removed by vacuum transfer. A 100-mL sample of benzene was added to the mixture and warmed to 40 °C to dissolve the product. The solution was filtered and the benzene volume reduced to 25 mL. The resultant purple crystals were recrystallized twice to yield 2.0 g of dibenzylniobocene. The same methodology afforded $Cp_2Nb(CH_2C_6H_4OCH_3)_2$ in a similar yield. The ESR of these compounds displayed 10-line spectra with g values of 2.01 for both $Cp_2Nb(CH_2C_6H_5)_2$ and $Cp_2Nb(CH_2C_6H_4OCH_3)_2$ and Nb hyperfine couplings of 86 and 84 G, respectively. Cyclic voltammograms of the dibenzyl compounds were conducted in THF with 0.1 M tetrabutylammonium tetrafluoroborate. The reference potential was Ag/Ag^+ (0.01 M in CH_3CN). Peak to peak separations were 90 mV at 200-mV/s scan rate. These were considered reversible based on the identical peak to peak separation of added ferrocene at +0.2 V.[41] The redox potentials for $Cp_2Nb(CH_2C_6H_5)_2$ were −2.02 V for reduction and −0.62 V for oxidation relative to Ag/Ag^+. For $Cp_2Nb(CH_2C_6H_4OCH_3)_2$ the potentials were −2.12 and −0.79 V. Coulometry indicated 1.01 electrons per equivalent were consumed for the reduction of $Cp_2Nb(CH_2C_6H_5)_2$.

Preparation of $Cp_2Nb(CH_2Ph)(CO)$. A 810-mg sample of $Cp_2Nb(CH_2Ph)_2$ (2 mmol) was dissolved in 200 mL of THF. Four milliliters of 1% Na/Hg was added and the mixture stirred for 2 h until the solution was dark brown. This solution of dibenzyl anion was separated from the amalgam by decantation and filtration. A solution of 0.14 mL of CF_3CH_2OH in 20 mL of THF was added slowly over a period of 12 h to the anion solution under 1 atm of CO. The solvent was removed, and the benzyl carbonyl was extracted from the brown residue with 70 mL of warm octane. A green powder was isolated which was washed with cold pentane. A 375-mg sample of $Cp_2Nb(CH_2Ph)CO$ was obtained by sublimation of the green powder at 90 °C (10^{-3} torr) (55% yield).

Preparation of $Cp_2(H)Nb{=}CHOZr(H)Cp^*_2$. General Syntheses. A 1.0-g sample of $Cp_2Nb(H)(CO)$ (4 mmol) and 1.6 g of $Cp^*_2ZrH_2$ were added to 30 mL of toluene. The resulting orange solution was filtered and toluene removed by vacuum transfer. The orange residue was suspended in pentane and filtered to yield 2.2 g of $Cp_2(H)Nb{=}CHOZr(H)Cp^*_2$ (90% yield). All zirconoxy carbene complexes were prepared in this manner and stored in the dark at −20 °C.

Preparation of $Cp_2(CO)NbCH_2OZr(H)Cp^*_2$. A 1.0-g (1.62 mmol) sample of $Cp_2(H)Nb{=}CHOZr(H)Cp^*_2$ was stirred in 35 mL of toluene with 1 atm of CO for 8 h at 45 °C. After the mixture was cooled and filtered, the solvent volume was reduced to about 8 mL. The green precipitate was recrystallized and washed with pentane. A 825-mg sample of $Cp_2(CO)NbCH_2OZr(H)Cp^*_2$ was isolated (80% yield).

Preparation of $Cp_2Nb(H)(PhC{\equiv}CPh)$. A 300-mg of Cp_2NbH_3[42] (1.33 mmol) and 230 mg of diphenylacetylene (1.3 mmol) were heated to 65 °C in toluene for 2 h. The brown reaction mixture was cooled to 35 °C and then filtered. Solvent removal resulted in a brown oil. A yellow powder results from the repeated addition and removal of pentane by vacuum transfer. This powder was recrystallized from 40 mL of octane, yielding 400 mg of $Cp_2Nb(H)(PhC{\equiv}CPh)$ in (75% yield). The ^1H NMR spectrum is identical with that for niobium-containing products of the carbene migratory insertion reactions 11, **12**, and 13.

Preparation of $Cp^*_2Zr(H)(OCH{=}CHPh)$. A 700-mg sample of $Cp_2(CH_2Ph)Nb{=}CHOZr(H)Cp^*_2$ (1 mmol) and 175 mg of diphenylacetylene (1 mmol) were stirred in toluene at 25 °C for 2 days. Toluene was removed by vacuum transfer. Several pentane addition–removal cycles yielded a tractable powder. Most of the zirconium enolate was extracted by filtration of a solution in 15 mL of pentane at 0 °C. The resultant yellow solution was reduced to 3 mL and cooled to −80 °C to form a colorless crystalline product. Cold filtration yielded 300 mg of *trans*-$Cp^*_2Zr(H)(OCH{=}CHPh)$ (62% yield).

A mixture of the *cis*- and *trans*-zirconium phenyl enolates was prepared by treating $Cp^*_2Zr(H)Cl$ with $NaOCH{=}CHPh$. An 80-mg sample of NaH (Alfa) was suspended in 80 mL of THF. A 0.35 mL solution of phenyl acetaldehyde (Aldrich) was added at −30 °C, and the mixture was allowed to react for 8 h at 25 °C. This solution was filtered onto 800 mg of $Cp^*_2Zr(H)Cl$ and stirred 4 h. The THF was removed and replaced with pentane. A yellow powder was isolated after filtration whose NMR showed both the *cis*- and *trans*-enolate hydrides in an approximate ratio of 1:1.

Kinetics of the Hydride Migration Promoted by CO. A typical experiment involved 40 mg of $Cp_2(H)Nb{=}CHOZr(H)Cp^*_2$ dissolved in 40 mL of benzene (16.2 mM) in a 10-mm quartz cell with a 50-mL total volume. The reaction was run at 22 °C under a measured CO pressure. The visible spectrum was recorded periodically as the reaction proceeded. The reaction was stirred between recordings but no significant deviation in the rate occurred without stirring. Plots of ln ($A_\infty - A$) at 600 nm vs. time were linear for 3 half lives. Plots of rate vs. CO pressure indicated a first-order CO dependence.

Kinetics of Hydrogen Exchange Using Saturation Transfer. The pulsing technique employed is described by Freeman.[43] The relaxation times for the protons of $Cp_2(H)Nb{=}CHOZr(H)Cp^*_2$ were measured by using the inversion recovery program of the JEOL FX90Q.[44] Saturation transfer spectra were obtained by using a pulse sequence program written by Perkins[45] which involves saturating a specific resonance and delaying the observation pulse a specified interval. A three-parameter nonlinear least-squares fit[46] of the difference in integrated intensities of the inverted

---

(34) (a) Marsella, J. A.; Curtis, C. J.; Bercaw, J. E.; Caulton, K. G. *J. Am. Chem. Soc.*, in press. (b) Labinger, J. A.; Komadina, K. *J. Organomet. Chem.* **1978**, *155*, C25.

(35) Marvich, R. H.; Brintzinger, H. H. *J. Am. Chem. Soc.* **1971**, *93*, 2046.

(36) Brown, T. L.; Dickerhoof, D. W.; Bafus, D. A.; Morgan, G. L. *Rev. Sci. Instrum.* **1962**, *33*, 491.

(37) Otto, E. E. H.; Brintzinger, H. H. *J. Organomet. Chem.* **1979**, *170*, 373.

(38) Manriquez, J. M.; McAlister, D. R.; Sanner, R. D.; Bercaw, J. E. *J. Am. Chem. Soc.* **1976**, *98*, 6733.

(39) Lucas, C. R. *Inorg. Synth.* **1976**, *16*, 107.

(40) McAlister, D. R.; Bercaw, J. E., unpublished results.

(41) Alexander, R.; Parker, A. J.; Sharp, J. H.; Waghorne, W. E. *J. Am. Chem. Soc.* **1972**, *94*, 1148.

(42) Labinger, J. A.; Wong, K. S. *J. Organomet. Chem.* **1979**, *170*, 373.

(43) Morris, G. A.; Freeman, R. *J. Magn. Reson.* **1978**, *29*, 433.

(44) "JEOL FS90Q Operation Manual", Chapter 6.

(45) Perkins, T., private communication.

resonance and the exchanging resonance as a function of delay time to the magnetization equation was performed on a Commodore Pet computer. $\partial(M_A - M_B)/\partial t = (M_A - M_B)/T_1 - 2k_{ex}(M_A - M_B)$, M_A and M_B are the inverted resonance and the exchanging peak magnitudes, respectively. T_1 is the average relaxation time of these two protons; k_{ex} equals the exchange rate.

Kinetic Measurements of Alkyl Migrations. The rates of alkyl migrations were followed by FT NMR. Less than 45° observation pulses were used. Repetition rates were at intervals greater than twice the relaxation times of the protons being measured. Reaction temperatures were maintained by the probe temperature controller and observed to be constant to within 1° by measuring the peak separations of ethylene glycol. A typical reaction involved 30 mg of $Cp_2(PhCH_2)Nb{=}CHOZr(H)Cp^*_2$ (42 μmol) and 30 mg of diphenylacetylene (170 μmol) dissolved in 0.45 mL of benzene-d_6. As the reaction proceeded, the Cp resonance of starting material lost intensity as the Cp resonance due to $Cp_2Nb(H)(PhC{\equiv}CPh)$ appeared. The plot of the decay of the integrated intensity of the Cp proton resonance of starting complex as a function of time showed first-order behavior for more than 3 half lives. The rate for benzyl migration was independent of $PhC{\equiv}CPh$ concentration over a 50-fold range. Most migration rates were studied with only a three-fold excess of $PhC{\equiv}CPh$ yet displayed first-order kinetics for at least 3 half-lives.

Benzyl Migration Crossover Experiment. A 25-mg sample each of $Cp_2(PhCD_2)Nb{=}CHOZr(H)Cp^*_2$ and $Cp_2(PhCH_2)Nb{=}CDOZr(D)(Cp^*\text{-}d_{15})_2$ were mixed with 30 mg of diphenylacetylene in benzene-d_6. The reaction was monitored by NMR. The olefinic proton at δ 5.73 appears as a singlet for $Cp^*_2Zr(H)(OCH{=}CDPh)$; no doublet which would indicate $Cp^*_2Zr(H)(OCH{=}CHPh)$ was observed.

Acknowledgment. This work has been supported by the National Science Foundation (Grant No. CHE-8004636), to whom grateful acknowledgment is made.

---

(46) Hull, W. E., Ph.D. Dissertation, Harvard University, 1975.

Hydrogen-Evolving Systems. 4. The Reduction of Molecular Nitrogen and of Other Substrates in the Vanadium(II)–Pyrocatechol System

Gerhard N. Schrauzer* and Miles R. Palmer

Contribution from the Department of Chemistry, University of California at San Diego, Revelle College, La Jolla, California 92093. *Received July 11, 1980*

Abstract: Reactions of molecular nitrogen and of other substrates with vanadium(II)–pyrocatechol complexes occur in two-electron steps at monomeric V(II) centers rather than by collective electron-transfer processes involving polynuclear clusters of vanadium(II)–pyrocatechol complexes. The reduction of acetylene, for example, obeys the stoichiometric equation $V^{II}PC + C_2H_2 + 2H^+ \rightarrow V^{IV}PC + C_2H_4$ at high substrate concentrations. At low concentrations of substrate acetylene or with less reactive substrates S, the overall reaction stoichiometries are expressed more closely by the equation $2V^{II}PC + S + 2H^+ \rightarrow 2V^{III}PC + H_2S$, primarily because of the concurrent side reaction $V^{II}PC + V^{IV}PC \rightarrow 2V^{III}PC$. In the absence of added reducible substrates, H_2 is evolved spontaneously according to the equation $2V^{II}PC + 2H^+ \rightarrow 2V^{III}PC + H_2$. The reduction of N_2 to NH_3 occurs in a stepwise fashion with N_2H_2 and N_2H_4 as the intermediates. The high reduction potential of N_2 to N_2H_2 and the tendency of N_2H_2 to decompose into the elements are mainly responsible for the extreme dependence of the yields of NH_3 on pH and solvent.

In recent papers of this series[1,2] we reported on the reduction of nitrogen and of other substrates in heterogeneous systems containing vanadium(II) hydroxide in inert host matrices such as $Mg(OH)_2$ or $ZrO_2(aq)$. The reduction of N_2 with $V(OH)_2/Mg(OH)_2$ was originally shown by Shilov and his coworkers to yield hydrazine and ammonia,[3] and it was postulated that N_2 is reduced directly in clusters of two or four V(II) ions situated in the $Mg(OH)_2$ lattice.[4] However, other workers pointed out that such a reaction would be thermodynamically improbable.[5]

Our work established[1,2] that vanadium(II)-hydroxide acts as a 2-electron reductant and that the reduction of nitrogen to hydrazine takes place in a stepwise manner with the intermediate formation of diimide, N_2H_2, which disproportionates inside the host lattice into hydrazine and nitrogen.

Nikonova et al[6] reported in 1972 that complexes of V(II) with pyrocatechol (PC, 1,2-dihydroxybenzene) reduce molecular nitrogen to ammonia. The reaction was proposed[7-10] to proceed via a "collective four-electron-transfer mechanism" involving aggregates of two or four $V^{II}PC$ complexes which bind N_2 and reduce it directly to hydrazine. However, the existence of higher order $V^{II}PC$ complexes has not been adequately demonstrated, and no evidence for the collective four-electron-transfer mechanism of N_2 reduction has thus far been obtained.

We became interested in the reactions of N_2 with $V^{II}PC$ complexes because N_2 reduction is accompanied by a simultaneous production of hydrogen. At high N_2 pressures, the reaction stoichiometry has been given in terms of reaction 1.[7] Equation

$$N_2 + 8e^- + 8H^+ \rightarrow 2NH_3 + H_2 \qquad (1)$$

---

(1) Zones, S. I.; Vickrey, T. M.; Palmer, J. G.; Schrauzer, G. N., *J. Am. Chem. Soc.* **1976**, *98*, 7289.

(2) Zones, S. I.; Palmer, M. R.; Palmer, J. G.; Doemeny, J. M.; Schrauzer, G. N. *J. Am. Chem. Soc.* **1978**, *100*, 2113.

(3) Denisov, N. T.; Efimov, O. N.; Shuvalova, N. I.; Shilova, A. K.; Shilov, A. E. *Zh. Fiz. Khim.* **1970**, *44*, 2694.

(4) Denisov, N. T.; Shuvalova, N. I.; Shilov, A. E. *Kinet. Katal.* **1973**, *14*, 1325.

(5) Lorenz, B.; Möbius, G.; Rummel, S.; Wahren, M. *Z. Chem.* **1975**, *15*, 241.

(6) Nikonova, L. A.; Ovcharenko, A. G.; Efimov, O. N.; Avilov, V. A.; Shilov, A. E. *Kinet. Katal* **1972**, *13*, 1602.

(7) Nikonova, L. A.; Isaeva, S. A.; Pershikova, N. I.; Shilov, A. E. *J. Mol. Catal.* **1975**, *1*, 367.

(8) Ovcharenko, A. G.; Shilov, A. E.; Nikonova, L. A. *Isvest. Akad. Nauk, Ser. Khim.* **1975**, *3*, 534.

(9) Luneva, N. P.; Nikonova, L. A.; Shilov, A. E. *React. Kinet. Catal. Lett.* **1976**, *5*, 149.

(10) Luneva, N. P.; Nikonova, L. A.; Shilov, A. E. *Kinet. Katal.* **1977**, *18*, 254.